ACS Medicinal Chemistry Letters
Cite This: ACS Med. Chem. Lett. XXXX, XXX, XXX−XXX
Letter
pubs.acs.org/acsmedchemlett

^{18}F-Labeled PET Probe Targeting Enhancer of Zeste Homologue 2 (EZH2) for Cancer Imaging

Lihai Yu,[†] Nikola Despotovic,[‡] Michael S. Kovacs,[§,∥,▽] Christopher L. Pin,[*,‡,⊥,○] and Leonard G. Luyt[*,†,§,#]

[†]London Regional Cancer Program, 800 Commissioners Road East, London, Ontario N6A 5W9, Canada
[‡]Department of Physiology and Pharmacology, [§]Medical Imaging, [∥]Medical Biophysics, [⊥]Paediatrics, and [#]Chemistry, The University of Western Ontario, London, Ontario N6A 3K7, Canada
[▽]Medical Imaging and [○]Children's Health Research Institute, Lawson Health Research Institute, London, Ontario N6A 4V2, Canada

Supporting Information

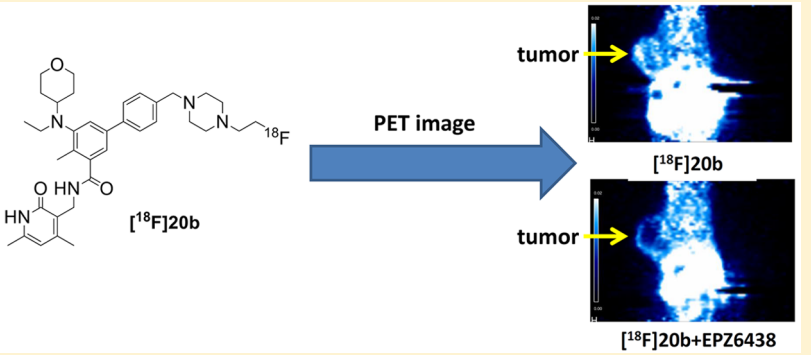

ABSTRACT: The enzyme enhancer of zeste homologue 2 (EZH2) plays a catalytic role in histone methylation (H3K27me3), one of the epigenetic modifications that is dysregulated in cancer. The development of a positron emission tomography (PET) imaging agent targeting EZH2 has the potential to provide a method of stratifying patients for epigenetic therapies. In this study, we designed and synthesized a series of fluoroethyl analogs based upon the structure of EZH2 inhibitors UNC1999 and EPZ6438. Among the candidate compounds, **20b** exhibited a high binding affinity to EZH2 (IC_{50} = 6 nM) with selectivity versus EZH1 (IC_{50} = 200 nM) by SAM competition assay, and furthermore, EZH2 inhibition was demonstrated in the pancreatic cancer cell line PANC-1 (IC_{50} = 9.8 nM). [^{18}F]**20b** was synthesized successfully and showed 5-fold higher uptake in PANC-1 cells than in MCF-7 cells. MicroPET imaging in a PANC-1 cell xenograft mouse model indicates that [^{18}F]**20b** has specific binding to EZH2, which was identified by *ex vivo* Western blot analysis of the tumor tissue.

KEYWORDS: *Enhancer of zeste homologue 2 (EZH2), fluorine-18, positron emission tomography (PET), pancreatic cancer, epigenetics*

Epigenetics is the study of factors that promotes heritable changes in gene expression without mutation to the primary DNA sequence. Epigenetic changes typically involve alterations to the DNA, the histones that make up the nucleosome core around which DNA is wrapped, or noncoding RNA transcripts that interact with mRNA or DNA. Epigenetic processes play essential roles in development and disease, and in the past decade, aberrant expression and activity of epigenetic regulating proteins have been described for many diseases including most cancers. Based on these observations, inhibition of cancer-relevant histone modifications has become a potential strategy for mono- or combinatorial cancer therapy. One particularly attractive epigenetic target is enhancer of zeste homologue 2 (EZH2), which is part the polycomb repressive complex 2 (PRC2) along with suppressor of zeste 12 (SUZ12) and embryonic ectoderm development (EED). EZH2 is expressed at very low levels in nonproliferating tissue yet increases during cancer progression, with high levels of EZH2 demonstrated in different cancer tissues such as prostate cancer, breast cancer, and pancreatic cancer.[1−3] In addition, gain of function mutants for EZH2 have been identified in a number of cancers including lymphomas. Importantly, increased EZH2 expression is not observed in all tumors, even from the same cancer type, suggesting some stratification of patients should be performed before therapeutic targeting of this protein.

EZH2 carries the catalytic activity for PRC2[4,5] required for trimethylation of lysine 27 on histone 3 (H3K27me3), which is

Received: December 6, 2018
Accepted: February 21, 2019

DOI: 10.1021/acsmedchemlett.8b00613
ACS Med. Chem. Lett. XXXX, XXX, XXX−XXX

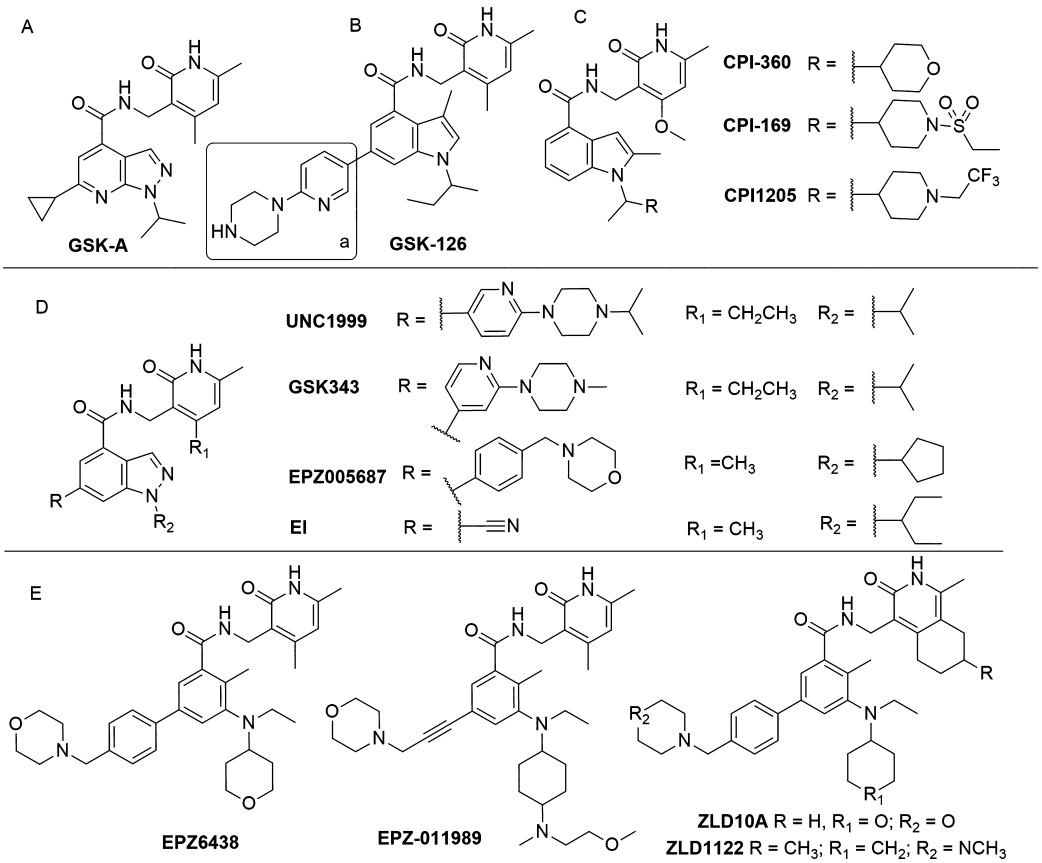

Figure 1. Structures of previous published EZH2 inhibitors.

mis-regulated in various cancers. Through this epigenetic modification, PRC2 promotes gene repression. The SET domain in the EZH2 sequence provides the active methyl group from the methyl group donor *S*-adenosyl-L-methionine (SAM) for H3K27me3. The gain of function EZH2 mutations observed in some cancers correlate with increased H3K27me3. Therefore, inhibition of the SET domain in EZH2 is a promising strategy for the cancer treatment, and several SAM-competitive EZH2 inhibitors with low IC_{50} value have been reported (Figure 1). GSK-A (Figure 1A) was first identified as an EZH2-binding chemical scaffold through a high throughput screening assay.[6] GSK-A contains both pyridone and 1*H*-pyrazolo[3,4-*b*]pyridine rings. Based on modifications to GSK-A's structure, a series of successful inhibitors with high affinity to EZH2 (nanomolar range) and high selectivity against EZH1 have been developed, including EPZ005684, UNC1999, GSK343, and E1 (Figure 1D).[7−10] We chose to target EZH2-specific inhibitors for developing diagnostic molecules since EZH2 has been more commonly linked to cancer progression than EZH1 and is the predominant methyltransferase in PRC2. In addition, while EZH2 expression is typically low in nonproliferative cells and tissues, EZH1 expression is readily detectable in adult tissues including skeletal muscle and salivary glands, which may increase imaging background. With the replacement of a pyridine ring with an indole ring, GSK126 (Figure 1B) was first developed in 2012, exhibiting high affinity to EZH2 (K_i = 0.5−3 nM) and selectivity compared to EZH1 (K_i = 89 nM).[11] The binding affinity was maintained by removing 1-(pyridin-2-yl)piperazine group from the indole ring and adding a series of six-membered rings on *N*-indole in CPI169, CPI360, and CPI1205 (Figure 1C).[12−14] GSK126 proceeded into clinical trials for lymphomas but ultimately was terminated.[15] The substitution of a methyl group with a methoxy group in the sensitive pyridine moiety maintains EZH2 inhibition activity. Based on a similar modification used for GSK126, another series of indazole analogs (Figure 1D) was successfully developed with a high retention of bioactivity to EZH2. By replacing 1*H*-pyrazolo[3,4-*b*]pyridine ring by aniline, EPZ6438 (Figure 1E) exhibited a 10-fold higher affinity to EZH2 (K_i = 2.5 nM) than the similarly structured EPZ005684 and 35-fold selectivity against EZH1.[16] EPZ6438 (Tazemetostat) has also proceeded into clinical trials for non-Hodgkin's lymphoma, and these studies are ongoing.[17] In addition, a series of promising compounds, including EPZ011989, ZLD10A, and ZLD1122, were recently described.[18−20]

While much progress has been made in developing EZH2 inhibitors for therapy, there are no reports of using these compounds for cancer diagnosis. The success in developing *in vivo* molecular imaging agents for detecting histone deacetylases (HDAC), for example, using the PET agent FAHA, suggests that epigenetic reprogramming proteins can be targeted for imaging purposes.[21] Positron emission tomography (PET), like CT or MRI, is a noninvasive imaging technique widely used to assist clinical diagnosis with the advantage of exceptionally good sensitivity and the ability for quantification. The goal of this study was to develop novel ^{18}F-labeled PET radiotracers specifically targeting EZH2 to allow for clinical cancer diagnosis and patient stratification.

Since both EPZ6438 and UNC1999 exhibit high binding affinity and selectivity for EZH2, we initially focused on modifying these inhibitors in order to develop PET imaging

DOI: 10.1021/acsmedchemlett.8b00613
ACS Med. Chem. Lett. XXXX, XXX, XXX−XXX

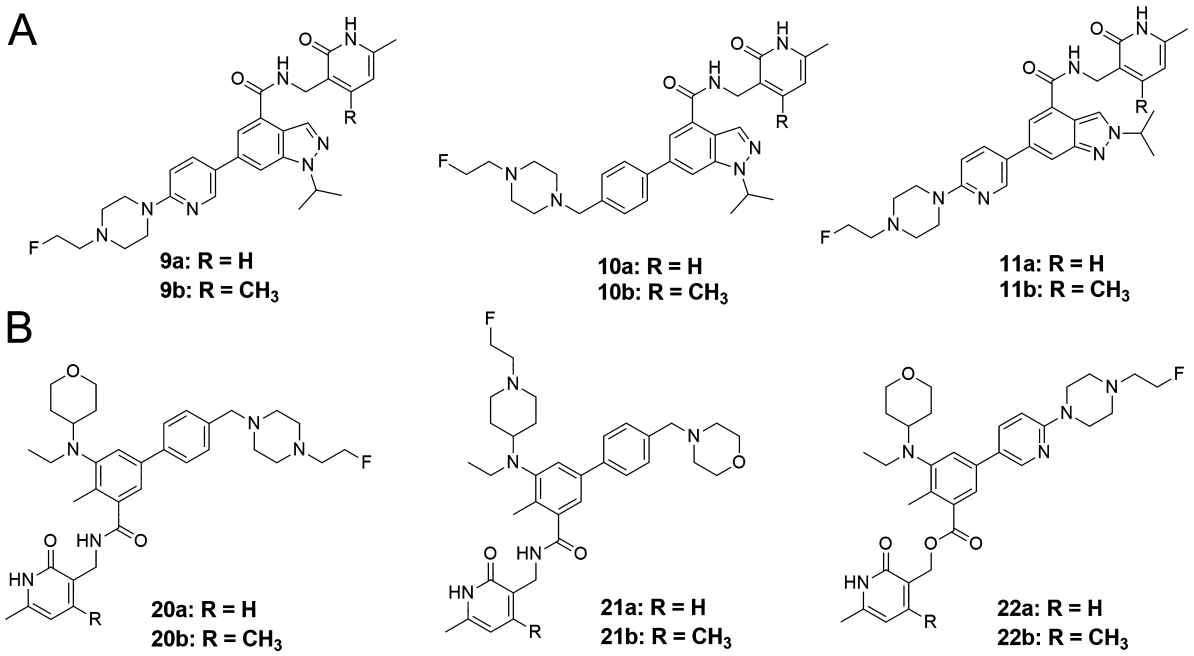

Figure 2. Structures of EZH2 inhibitor analogs designed and synthesized in this study: (A) UNC1999 series and (B) EPZ6438 series.

agents. Based on SAR studies regarding EZH2 inhibitors, we maintained the pharmacophore of pyridone, indazole, or aniline rings to retain biologically relevant features.[22] Considering the chemical framework of EPZ6438 and UNC1999, we designed modifications for side substitution on the indazole or aniline rings and/or removal of one alkyl group in position 4 of pyridone. Since [^{18}F]fluoroethyltosylate is a widely used intermediate in the development of PET tracers and can be coupled to secondary amines in radiosynthesis, fluoroethyl groups were introduced into piperidine in our target compounds. This provides a synopsis of the rationale behind the development of the corresponding radiotracers.

Based on this design strategy, 12 new compounds were synthesized as shown in Figure 2, with experimental details and synthetic schemes found in the Supporting Information. We initially assessed their binding to EZH2 using a cell-free competition assay for SAM that also suggests biological activity. The binding results compare the ability of these new compounds to inhibit PRC2 binding to SAM and are summarized in Table 1, including calculated Log P values. Six compounds (**9a**, **9b**, **10a**, **10b**, **11a**, and **11b**) share the same core structure with UNC1999 (Figure 2A). Pyridone has been accepted as an active moiety to occupy the SAM-binding pocket in EZH2 protein and is thus retained in this series. Compound **9b** displays the lowest IC_{50} value (0.1 μM) for EZH2 inhibition among the modified UNC-1999 compounds and a high selectivity versus EZH1, with 90-fold difference in IC_{50} value. Compared to compound **9b**, compound **9a** was found to have a higher IC_{50} (0.8 μM), which demonstrates that the replacement of methyl group by hydrogen in position 4 on the pyridine ring decreased the compound's interaction with EZH2, which is consistent with SAR analysis published by Yang.[22] Extending the fluorine-piperidine substituent one methylene away from the core (**10a**) resulted in a loss of affinity, as did relocation of the isopropyl substituent on the indazole (**11a**).

Table 1. Bioactivity of Compounds to EZH2 and Selectivity versus EZH1

compound	IC_{50} (EZH2)	IC_{50} (EZH1)	c Log P
9a	0.8 μM		1.98
9b	0.1 μM	9 μM	2.57
10a	1.3 μM	>10 μM	1.84
11a	8.5 μM		1.86
20a	30 nM		0.47
20b	6 nM	200 nM	1.06
21a	36 nM		0.61
21b	7 nM	280 nM	1.20
22a	74 nM		1.16
22b	8 nM	450 nM	1.75
GSK343	5–9 nM	1200 nM	
EPZ6438	15 nM (2.5 nM[16])		

Six fluorine-containing EPZ6438 analogs were prepared as indicated in Figure 2B. The oxygen atom in tetrahydropyran or morpholine of EPZ6438 was replaced by *N*-fluoroethyl group to obtain compounds **20b** and **21b**, respectively. Both **20b** and **21b** exhibit highly competitive activity against EZH2 at nanomolar levels similar to the EPZ6438 reference (IC_{50} = 15 nM). Replacement of the benzyl group in the pyridine ring, **22b**, maintains high binding. As a result, the modification on the boundary site of EPZ6438 with a fluoroethyl group does not affect EPZ6438 affinity to the SAM-competitive binding site. The IC_{50} values of **20b**, **21b**, and **22b** are more than 30-fold higher to EZH1 than to EZH2, which indicates these three compounds have high selectivity for EZH2. Finally, the replacement of 4,6-dimethylpyridin-2(1*H*)-one with 6-methylpyridin-2(1*H*)-one in **20a**, **21a**, and **22a** decreased biological activity based on competition assays. This is similar to the effect seen between **9a** and **9b** based upon the presence of a methyl group.

To examine cell uptake and maintenance of biological activity in cells, we examined the effects of these compounds on global H3K27me3 enrichment in histones isolated from

DOI: 10.1021/acsmedchemlett.8b00613
ACS Med. Chem. Lett. XXXX, XXX, XXX−XXX

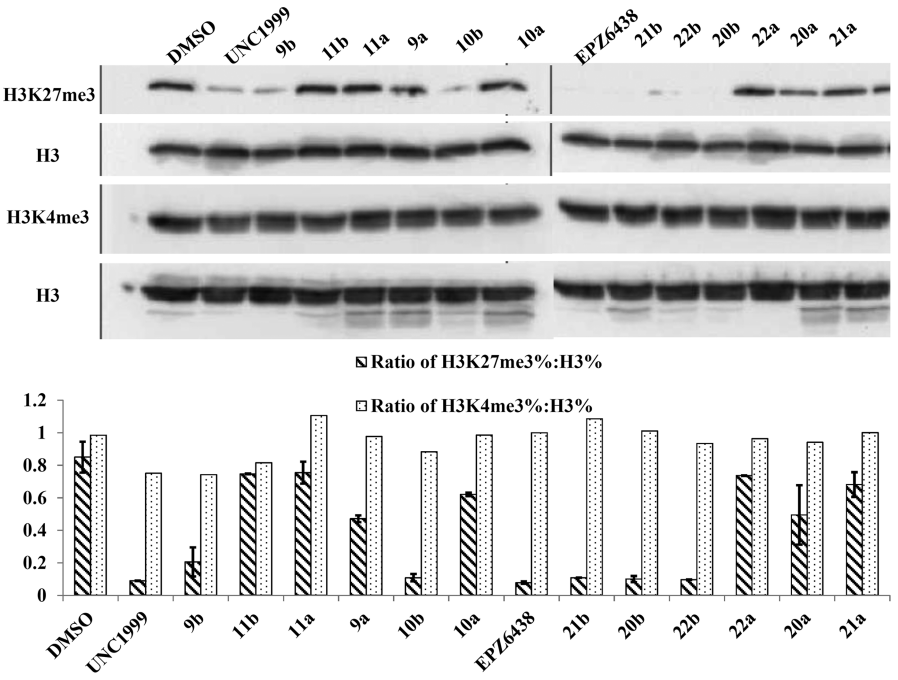

Figure 3. Effect of UNC1999 and EPZ6438 compounds on EZH2 activity in PANC-1 cells. Representative Western blot analysis for H3K27me3 or H3K4me3 on histone extracts from PANC-1 cells treated with UNC1999, EPZ6438, or modified compounds for 3 days. All blots were stripped and reprobed to assess the loading control, histone 3 (H3). Cell culture experiments were performed twice (n = 2) for H3K27me3 and once (n = 1) for H3K4me3. Bars represent mean ± standard deviation. No statistical analysis was performed on this data.

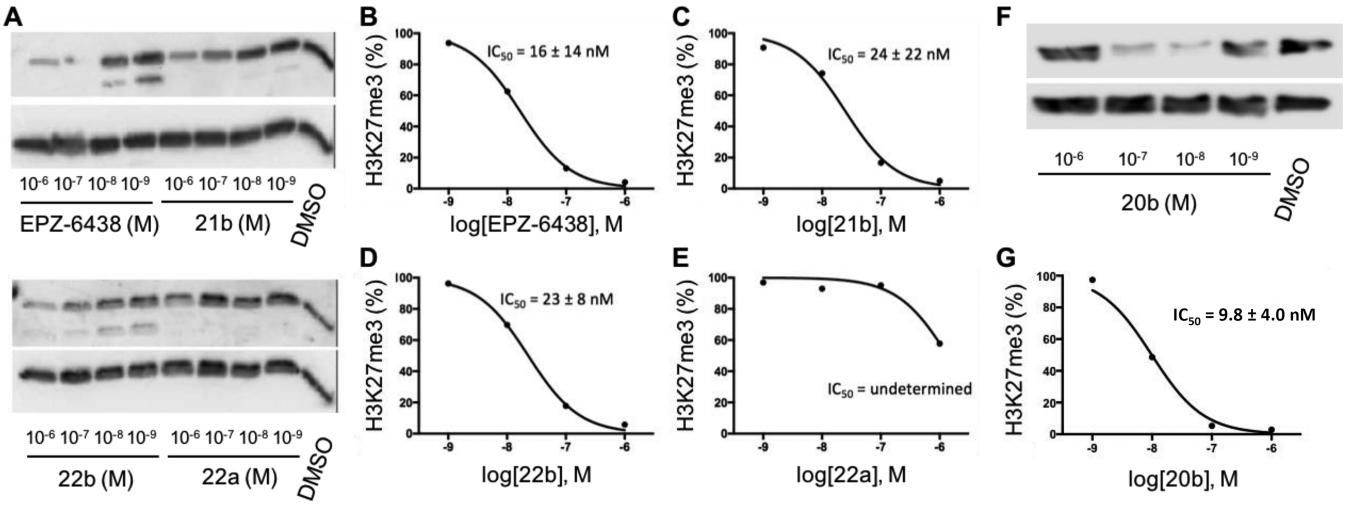

Figure 4. Increasing concentrations of EPZ6438, **20b**, **21b**, **22a**, and **22b** on H3K27me3 in PANC-1 cells. (A) Representative Western blot analysis for H3K27me3 on histone extracts from PANC-1 cells treated with increasing amounts of **21b**, **22a**, and **22b** for 3 days. All blots were stripped and reprobed to assess the loading control, histone 3 (H3). Inhibition curves for (B) parental EPZ6438, and compounds (C) **21b**, (D) **22b**, and (E) control **22a**. The % H3K27me3 represents the amount of H3K27me3:H3 relative to each blot's DMSO control. IC_{50} values, if applicable, are listed on their corresponding curve. There was no significant difference (p = 0.5795) between EPZ6438 and **21a**'s abilities to inhibit EZH2 activity. Similar Western blot analysis (F) and inhibition curves (G) for lead compound **20b**.

PANC-1 cells. PANC-1 cells are originally derived from a pancreatic ductal adenocarcinoma patient and exhibit high levels of EZH2 expression and H3K27me3. The relative ratio of H3K27me3-to-H3 densiometry (H3K27me3:H3) was used as a marker of EZH2 activity. PANC-1 cells exposed to 1 μM UNC1999 (0.089 ± 0.2%), **9b** (0.21 ± 9%), or **10b** (0.11 ± 2%) displayed a reduction in EZH2 activity relative to DMSO-treated cells (0.85 ± 9%) based on H3K27me3:H3 ratios. Other UNC1999-derived compounds showed a loss of EZH2 inhibition ability (Figure 3). No differences were observed for the non-EZH2 target H3K4me3. Similar analysis of the parental EPZ6438 and related compounds revealed maintained EZH2 inhibition for compounds **21b** (0.11 ± 0.001), **20b** (0.1 ± 0.02), and **22b** (0.1 ± 0.002) similar to EPZ6438 (0.08 ± 0.008). These levels of EZH2 activity are significantly lower (p < 0.0001) in PANC-1 cells compared to DMSO control (0.84 ± 0.1).

From this data, compounds **20b**, **21b**, **22a**, and **22b** were selected for dose-dependent analysis (Figure 4). EPZ6438 was selected for use as a positive control; **20b**, **21b**, and **22b** as

DOI: 10.1021/acsmedchemlett.8b00613
ACS Med. Chem. Lett. XXXX, XXX, XXX−XXX

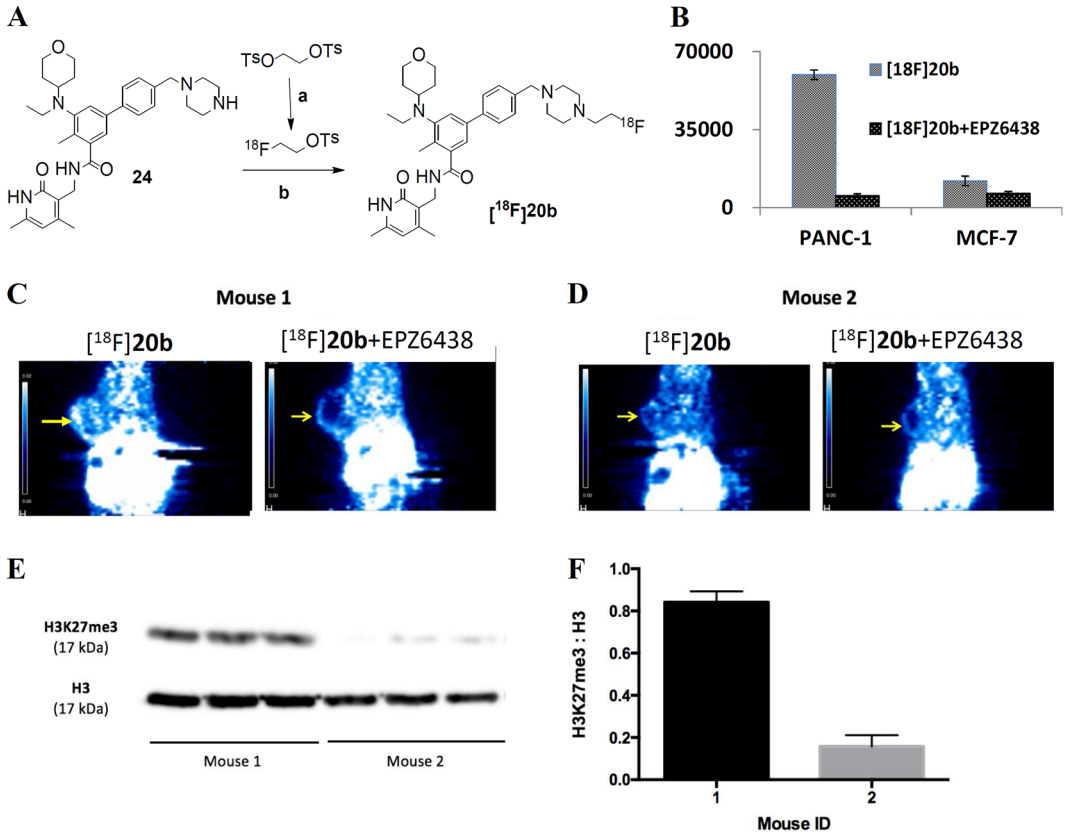

Figure 5. (A) Reagents and conditions: a. $K_{2.2.2}$, K_2CO_3, ACN, 115 °C, 10 min; b. K_2CO_3, ACN, 130 °C (MW), 10 min. (B) Cell uptake [^{18}F]**20b** (1 MBq) in 100 μL of PBS buffer, PANC-1, or MCF-7 cells (600,000 each vial) in 1 mL of incubation medium, n = 5, and EPZ6438 (100 μg) in 10 μL of DMSO. (C,D) Correlating EZH2 activity to PET signal intensity for mice with PANC-1 tumor. microPET image at 100−120 min in NOD/SCID mice (n = 2) with PANC-1 cells tumor xenografts were administered a 10 MBq IV dose of [^{18}F]**20b** and blocked by EPZ6438. (E,F) EZH2 expression in tumor tissue samples from PANC-1 tumors were analyzed by Western blots.

candidate compounds; and **22a** as the negative control. While UNC1999, **11b**, and **10b** displayed comparable EZH2 inhibition at 1 μM, they were not chosen for further study since the cell-free binding experiments (Table 1) suggested that they have much weaker binding affinities than their EPZ6438 counterparts. PANC-1 cells exposed to increasing concentrations of EPZ6438 (n = 3), **21b** (n = 3), **22b** (n = 2), and **20b** (n = 3) for 3 days were found to have IC_{50} values of 16 ± 14, 24 ± 22, 23 ± 8, and 9.8 ± 4.0 nM, respectively (Figure 4) indicating no significant difference (p = 0.5795) between the EZH2 inhibitory potential of EPZ6438 and the modified versions of this compound in PANC-1 cells. The IC_{50} for **22a** (n = 2) could not be calculated based on this concentration range. Combined, this data confirms that compounds **20b**, **21b**, and **22b** are taken up by tumor cells and maintain the ability to inhibit EZH2-mediated H3K27me3. Considering the biological data in Table 1 and the finding that compound **20b** has a lower Log P value than **21b** and **22b**, combined with evidence of superior EZH2 inhibition, we decided to proceed with the development of a radiosynthetic route for radiolabeling **20b** with the PET radioisotope ^{18}F to determine its potential as an *in vivo* imaging agent.

The radiosynthesis of [^{18}F]**20b** was accomplished by a two-step approach (Figure 5A). Aqueous [^{18}F]F$^-$ was dried under the presence of Kryptofix2.2.2. and K_2CO_3 by azeotropic drying. Ethylene di(p-toluenesulfonate) was reacted with dried [^{18}F]F$^-$/Kryptofix2.2.2 complex resulting in the [^{18}F]-fluoroethyltosylate prosthetic group, with a radiochemical yield of 34% (decay corr.) after purification by semipreparative HPLC. [^{18}F]Fluoroethyltosylate was coupled to the precursor compound **24**, which contains a secondary amine, in acetonitrile at 130 °C for 10 min. Purification by HPLC provided [^{18}F]**20b** in a yield of 25% (decay corr.). The total yield for two steps is 8.5% (decay corr.) with nonradioactive compound **20b** used as a reference compound to confirm the presence of [^{18}F]**20b** (Figure S1, Supporting Information). The specific activity is 10−25 GBq/μmol and radiopurity >95%. The partition coefficient (log P = 1.93) was measured in n-octanol/phosphate buffer. [^{18}F]**20b** was used to perform the following cell study.

EZH2 is overexpressed in various cancers, including pancreatic and breast cancers. Human pancreatic carcinoma cell (PANC-1) and human breast adenocarcinoma cell (MCF-7) are typical cell lines for pancreatic cancer and breast cancer. To determine if radiolabeled **20b** targets EZH2 at the tracer level in live cells, we investigated the uptake of [^{18}F]**20b** to target EZH2 in PANC-1 and MCF-7 cells. Since [^{18}F]**20b** is an analog of EPZ6438 and both have a similar affinity for EZH2, we used a large excess of EPZ6438 for a blocking study to test [^{18}F]**20b**'s specific binding affinity to EZH2 in PANC-1 and MCF-7 cells (Figure 5B). [^{18}F]**20b** exhibited 5-fold higher uptake in PANC-1 cells compared to MCF-7 cells. Coincubation of the radiotracer [^{18}F]**20b** with 100 μg of EPZ6438 reduced radioactivity accumulation in both PANC-1 and MCF-7 cells. [^{18}F]**20b** uptake decreased 90% lower in

DOI: 10.1021/acsmedchemlett.8b00613
ACS Med. Chem. Lett. XXXX, XXX, XXX−XXX

PANC-1 cells treated by EPZ6438 with a 50% reduction in MCF-7 cells. These results suggest that EZH2 is expressed to higher levels in PANC-1 cells compared to MCF-7 cells and confirms [^{18}F]**20b** exhibits specificity for EZH2 in a live cell situation. Therefore, we next examined [^{18}F]**20b**'s ability to identify EZH2 accumulation in animals.

As a pilot experiment for PET imaging, 3×10^6 PANC-1 cells were transplanted into NOD/SCID mice and imaging performed once tumors reached 0.8−1 cm in diameter. At this time, mice were imaged for 2 h using PET scanning. PET images show moderate tumor uptake (Figure 5C,D) when mice were administrated with 10 MBq [^{18}F]**20b**. While high background was observed in both mice, pretreatment with EPZ6438 resulted in decreased [^{18}F]**20b** uptake in the tumor suggesting that [^{18}F]**20b** selectively binds EZH2 protein *in vivo*. Surprisingly, [^{18}F]**20b** activity differed significantly between mice. To determine if this reflected differences in EZH2 activity, histones were isolated from PANC-1-derived tumors following imaging and assessed for global H3K27me3 levels (*ex vivo*). As suggested by the imaging results, the tumor displaying higher [^{18}F]**20b** uptake had significantly more H3K27me3 present, indicating higher EZH2 activity (Figure 5E, F). The correlation between tumor signal intensity and EZH2 activity suggests that *in vivo* EZH2 activity can be noninvasively imaged and quantified with [^{18}F]**20b**. However, the high level of background uptake for this PET agent indicates that further modifications to the imaging agent are required to make this approach clinically viable. Although the LogP value is reasonable for a small molecule, the high liver uptake suggests that a further lowering of LogP may be helpful, as well as studies to investigate *in vivo* stability. For example, the addition of a PEG chain to **20b** could decrease background in the PET images by reducing its lipophilicity.

Conclusion. A fluorine containing analogue of EPZ6438, [^{18}F]**20b**, was discovered to exhibit high binding affinity to EZH2 protein *in vitro*, inhibit H3K27me3 methylation in cells, and selectively label EZH2 protein in PANC-1-derived xenograft tumors. Currently, [^{18}F]**20b** is not suitable for clinical diagnosis due to high background uptake of the imaging agent but will need to be further modified to reduce background. However, PET imaging and Western blot analysis demonstrates that [^{18}F]**20b** or derivatives of this compound optimized for pharmacokinetic behavior may be used to stratify the expression of EZH2 in patients and noninvasively determine epigenetic methylation status (H3K27me3) *in vivo*. New PET tracers based on further chemical modifications to the parent EPZ6438 will be investigated in the future.

■ ASSOCIATED CONTENT

Supporting Information

The Supporting Information is available free of charge on the ACS Publications website at DOI: 10.1021/acsmedchemlett.8b00613.

Procedures for the synthesis of all candidate compounds with chemical structural characterization, methods for binding affinity screening using SAM-competing assay and cell inhibition study, synthetic schemes for all compounds, and HPLC chromatograms for **20b** and [^{18}F]**20b** (PDF)

■ AUTHOR INFORMATION

Corresponding Authors

*Tel: 519-685-8600 ext. 53302. E-mail: lluyt@uwo.ca.

*Tel: 519-685-8500 ext. 53073. Fax: 519-685-8156. E-mail: cpin@uwo.ca.

ORCID

Leonard G. Luyt: 0000-0002-0941-4731

Author Contributions

The manuscript was written through contributions of all authors. All authors have given approval to the final version of the manuscript.

Funding

This work was supported by the Cancer Research Society with funding through an operating grant titled "Targeting enhancer of Zeste 2 (EZH2) for non-invasive cancer imaging".

Notes

The authors declare no competing financial interest.

■ ACKNOWLEDGMENTS

The authors wish to thank Dr. Ting-Yim Lee and his staff for providing access to small animal imaging equipment.

■ ABBREVIATIONS

EZH2, enhancer of zeste homologue 2; PET, positron-emission tomography

■ REFERENCES

(1) Chervona, Y.; Costa, M. Histone modifications and cancer: biomarkers of prognosis? *Am. J. Cancer Res.* **2012**, *2*, 589−597.

(2) Yoo, K. H.; Hennighausen, L. EZH2Methyltransferase and | H3K27 Methylation in breast cancer. *Int. J. Biol. Sci.* **2012**, *8*, 59−65.

(3) Ougolkov, A. V.; Bilim, V. N.; Billadeau, D. D. Regulation of pancreatic tumor cell proliferation and chemoresistance by the histone methyltransferase enhancer of zeste homologue 2. *Clin. Cancer Res.* **2008**, *14*, 6790−6796.

(4) Cao, R.; Zhang, Y. The functions of E(Z)/EZH2-mediated methylation of lysine 27 in histone H3. *Curr. Opin. Genet. Dev.* **2004**, *14*, 155−164.

(5) Cao, R.; Wang, L.; Wang, H.; Xia, L.; Erdjument-Bromage, H.; Tempst, P.; Jones, R. S.; Zhang, Y. Role of histone H3 lysine 27 methylation in polycomb-group silencing. *Science* **2002**, *298*, 1039−1043.

(6) Diaz, E.; Machutta, C. A.; Chen, S. Development and validation of reagents and assays for EZH2 peptide and nucleosome high-throughput screens. *J. Biomol. Screening* **2012**, *17*, 1279−1292.

(7) Knutson, S. K.; Wigle, T. J.; Warholic, N. M.; et al. A selective inhibitor of EZH2 blocks H3K27 methylation and kills mutant lymphoma cells. *Nat. Chem. Biol.* **2012**, *8*, 890−896.

(8) Konze, K. D.; Ma, A.; Li, F.; et al. An orally bioavailable chemical probe of the lysine methyltransferases EZH2 and EZH1. *ACS Chem. Biol.* **2013**, *8*, 1324−1334.

(9) Verma, S. K.; Tian, X.; Lafrance, L. V.; et al. Identification of potent, selective, cell-active inhibitors of the histone lysine methyltransferase EZH2. *ACS Med. Chem. Lett.* **2012**, *3*, 1091−1096.

(10) Qi, W.; Chan, H.; Teng, L.; et al. Selective inhibition of EZH2 by a small molecule inhibitor blocks tumor cells proliferation. *Proc. Natl. Acad. Sci. U. S. A.* **2012**, *109*, 21360−21365.

(11) McCabe, M. T.; Ott, H. M.; Ganji, G.; et al. EZH2 inhibition as a therapeutic strategy for lymphoma with EZH2-activiting mutations. *Nature* **2012**, *492*, 108−112.

(12) Gehling, V. S.; Vaswani, R. G.; Nasveschuk, C. G.; et al. Discovery, design, and synthesis of indole-based EHZ2 inhibitors. *Bioorg. Med. Chem. Lett.* **2015**, *25*, 3644−3649.

DOI: 10.1021/acsmedchemlett.8b00613
ACS Med. Chem. Lett. XXXX, XXX, XXX−XXX

(13) Bradley, W. D.; Arora, S.; Busby, J.; et al. EZH2 inhibitor efficacy in non-hodgkin's lymphoma does not require suppression of H3K27 monomethylation. *Chem. Biol.* **2014**, *21*, 1463−1475.
(14) Vaswani, R. G.; Gehling, V. S.; Dakin, L. A.; et al. Identification of (R)-N-((4-methoxy-6-methyl-2-oxo-1,2-dihydropyridin-3-yl)-methyl)-2-methyl-1-(1-(1-(2.2.2-trifluoroethyl)piperidin-4-yl)ethyl-1H-indole-3-carboxamide (CPI-1205), a potent and selective inhibitor of histone methyltransferase EZH2, suitable for phase I clinical trials for B-cell lymphomas. *J. Med. Chem.* **2016**, *59*, 9928−9941.
(15) A study to investigate the safety, pharmacokinetics, pharmacodynamics and clinical activity of GSK2816126 in subjects with relapsed/refractory diffuse large B cell lymphoma, transformed follicular lymphoma, other non-Hodgkin's lymphomas, solid tumors and multiple myeloma. https://clinicaltrials.gov/ct2/show/NCT02082977 (accessed 21 Aug 2018).
(16) Knutson, S. K.; Warholic, N. M.; Wigle, T. J.; et al. Durable tumor regression in genetically altered malignant rhabdoid tumors by inhibition of methyltransferase EZH2. *Proc. Natl. Acad. Sci. U. S. A.* **2013**, *110*, 7922−7927.
(17) Italiano, A.; Soria, J. C.; Toulmonde, M.; et al. Tazemetostat, an EZH2 inhibitor, in relapsed or refractory B-cell non-Hodgkin lymphoma and advanced solid tumours: a first-in-human, open-label, phase 1 study. *Lancet Oncol.* **2018**, *19*, 649−659.
(18) Campbell, J. E.; Kuntz, K. W.; Knutson, S. K.; et al. EPZ011989, A potent, orally-available EZH2 inhibitor with robust in vivo activity. *ACS Med. Chem. Lett.* **2015**, *6*, 491−495.
(19) Song, X.; Zhang, L.; Gao, T.; et al. Selective inhibition of EZH2 by ZLD10A blocks H3K27 methylation and kills mutant lymphoma cells proliferation. *Biomed. Pharmacother.* **2016**, *81*, 288−294.
(20) Gao, T.; Zhang, L.; Zhu, Y.; et al. ZLD1122, A novel EZH2 and EZH1 small molecular inhibitor, blocks H3K27 methylation and diffuse large B cell lymphoma cell growth. *RSC Adv.* **2016**, *6*, 28512−28521.
(21) Fukumitsu, N.; Yeh, S.; Flores, L.; et al. In vivo 6-([18F]fluoroacetamido)-1-hexanoicanilide PET imaging of altered histone deacetylase activity in chemotherapy-induced neurotoxicity. *Contrast Media Mol. Imaging* **2018**, *3*, 1−12.
(22) Yang, X.; Li, F.; Konze, K. D.; et al. Structure-activity relationship studies for enhancer of zeste homologue 2 (EZH2) and enhancer of zeste homologue 1 (EZH1) inhibitors. *J. Med. Chem.* **2016**, *59*, 7617−7633.

DOI: 10.1021/acsmedchemlett.8b00613
ACS Med. Chem. Lett. XXXX, XXX, XXX−XXX